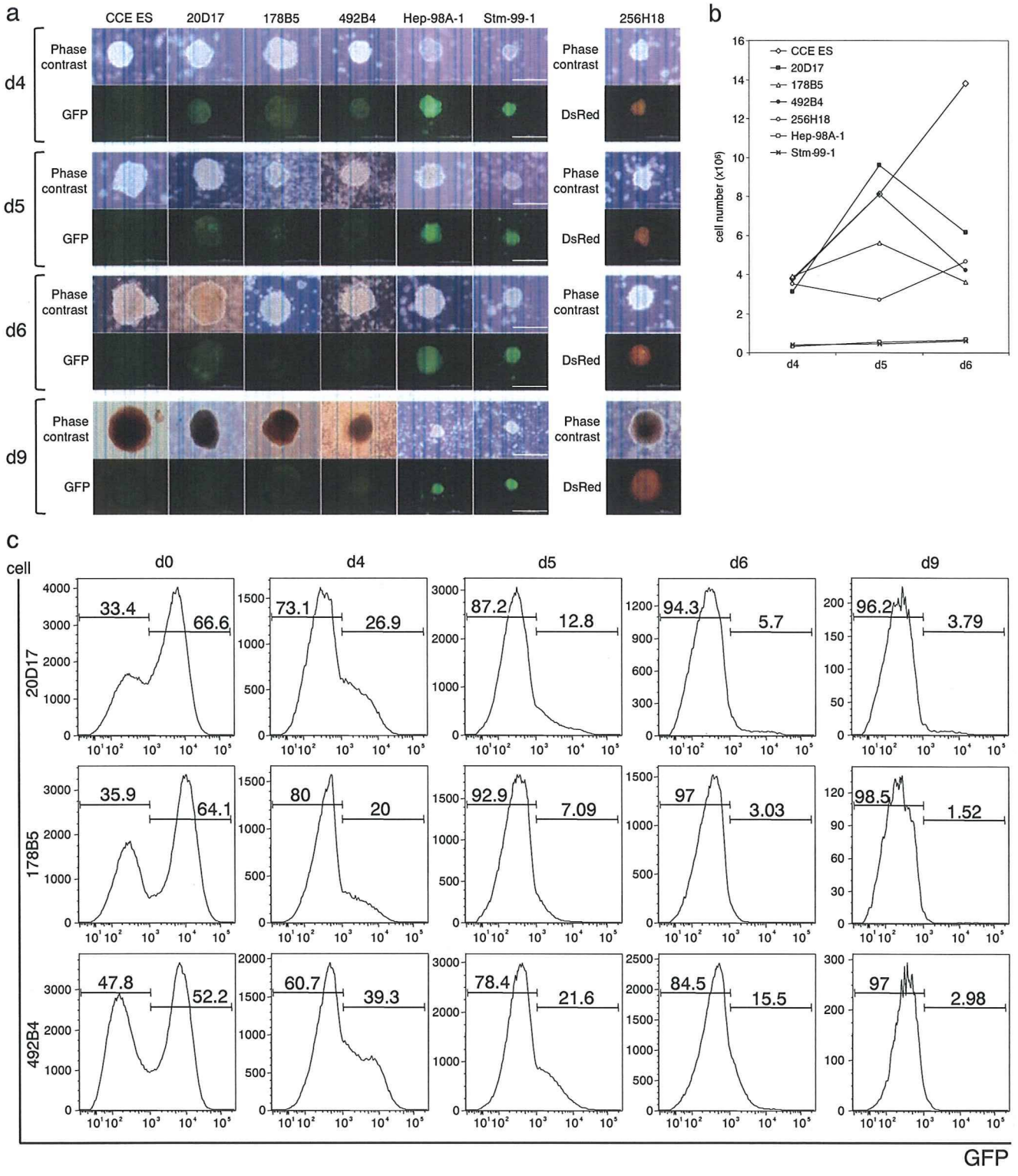

Fig. 2 Proliferation and differentiation of CCE ES and iPS cells. **a** Morphology of EBs at days (d) 4, 5, and 6. Scale bars on days 4 to 6 are 200 μm, while on day 9 it is 400 μm. **b** Total number of differentiated ES/iPS cells during formation of EBs at days 4, 5, and 6. **c** Decrease in Nanog-GFP expression during EB formation of MEF-derived iPS cells (lines 20D17, 178B5, and 492B4). Shown is the percentage of GFP-negative and -positive cells (first and second peak, respectively) at days 0 (before EB formation), at days 4, 5, 6, and 9 of EB formation

20D17, 178B5, and 492B4 iPS cells was identical to that of CCE ES cells, while EBs from 256H18, Hep-98A-1, and Stm-99-1 iPS cells were relatively smaller than those from other iPS lines (Fig. 2a). In addition to size, Hep-98A-1 and Stm-99-1 iPS cells yielded a lower number of EBs; specifically, with those lines the number of CCE ES cells gradually increased from days 4 to 6, while the number of 20D17, 178B5, and 492B4 iPS cells increased from days 4 to 5 of culture and then decreased at day 6 (Fig. 2b). By contrast to MEF-derived iPS cells, the number of 256H18 iPS cells slightly decreased from days 4 to 5 and then increased at day 6 (Fig. 2b). The number of Hep-98A-1 and Stm-99-1 iPS cells was overall lower than that from other lines and slightly increased from days 4 to 6 (Fig. 2b). These observations suggest that in the same culture conditions, different iPS lines exhibit differences in proliferation and capacity to form EBs.

Nanog-GFP activity of 20D17, 178B5, and 492B4 iPS cells was observed in EBs at day 4 and fluorescence decreased by day 6 of culture (Fig. 2a). Flow cytometry analysis indicated that Nanog-GFP-positive cells from 20D17, 178B5, and 492B4 iPS cells gradually decreased during EB formation and constituted a small proportion of cells (3.79%, 1.52%, and 2.98%, respectively, $p<0.05$) by culture day 9 (Fig. 2c). Taken together, our results indicate that MEF-derived 20D17, 178B5, and 492B4 iPS cells resemble CCE ES cells in terms of morphology in feeder-free cultures, number and size of EBs, and proliferation compared to adult-derived 256H18, Hep-98A-1, and Stm-99-1 iPS cells.

Generation of Mesodermal Cells from EBs

Blood cells have been generated from mesoderm marked by Flk1 [17, 18]. Thus, we compared the number of mesodermal cells (E-cadherin$^-$ Flk1$^+$) differentiated from iPS cell lines during the course of EB formation. It is reported that a high percentage of Flk1$^+$ mesodermal cells are obtained from EBs around days 4 to 4.5 [19, 20]. We extended this culture period in order to count the number of mesodermal cells from Hep-98A-1 and Stm-99-1 iPS cells, which proliferated more slowly than did other lines evaluated. The percentage and number of E-cadherin$^-$ Flk1$^+$ cells from CCE ES cells gradually decreased from days 4 to 6 (Fig. 3a, c, and Supplemental Fig. 1). This pattern was similarly observed in 20D17 and 178B5 iPS lines (Fig. 3a, c, and Supplemental Fig. 1). By contrast, the number of E-cadherin$^-$ Flk1$^+$ cells from 492B4, 256H18, Hep-98A-1, and Stm-99-1 iPS cells increased from days 4 to 5 and then decreased (Fig. 3a and c).

Mesodermal cells can be divided into two sub-populations: paraxial, which expresses platelet-derived endothelial growth factor receptor α (PDGFRα) and proximal lateral mesoderm, which does not. To determine which sub-populations are generated from each iPS line, we first compared the number of E-cadherin$^-$ PDGFRα$^+$ cells in various lines. From days 4 to 6, E-cadherin$^-$ PDGFRα$^+$ cells from CCE ES and 178B5 iPS cells gradually decreased, while E-cadherin$^-$ PDGFRα$^+$ cells from 20D17, 492B4, Hep-98A-1, and Stm-99-1 iPS cell lines increased from days 4 to 5 and then decreased (Fig. 3b and c). The number of E-cadherin$^-$ PDGFRα$^+$ cells from 256H18 iPS lines slightly decreased from days 4 to 6 (Fig. 3b and c). Relevant to the percentage of E-cadherin$^-$ PDGFRα$^+$ cells, two expression patterns were observed: 1) percentage of PDGFRα$^+$ cells from CCE ES, 20D17, and 178B5 iPS cells decreased from days 4 to 5 and then increased at day 6 (Supplemental Fig. 1), and 2) the percentage of PDGFRα$^+$ cells from 492B4, 256H18, Hep-98A-1, and Stm-99-1 iPS cells increased from days 4 to 5 and decreased at day 6 (Supplemental Fig. 1). Taken together, 20D17 and 178B5 iPS cells showed similar differentiation into E-cadherin$^-$ Flk1$^+$ mesodermal cells and E-cadherin$^-$ PDGFRα$^+$ paraxial lateral mesodermal cells to that of CCE ES cells, compared to other iPS lines.

Hematopoietic Potential of iPS Cells in EBs

Next we determined the percentage of HCs in EBs at day 9 of culture among iPS cell lines. In the presence of SCF, IL-3, and EPO, CCE ES cells differentiated into hematopoietic progenitors (c-Kit$^+$ CD45$^+$), myeloid cells (CD45$^+$) and erythroid cells (Ter119$^+$) at 0.45%, 25.9% and 3.85%, respectively ($p<0.05$) (Fig. 4a). No c-Kit$^+$ CD45$^+$ cells were generated from any iPS line. The percentage of CD45$^+$ and Ter119$^+$ cells varied among iPS cell lines. Specifically, the percentages of CD45$^+$ cells in iPS lines were Hep-98A-1 (1.37%), 256H18 (1.03%), Stm-99-1 (0.85%), 20D17 (0.69%), 178B5 (0.22%), and 492B4 (0.03%), and the percentages of Ter119$^+$ cells were 178B5 (3.35%), Hep-98A-1 (1.53%), Stm-99-1 (1.48%), 492B4 (0.39%), 20D17 (0.11%), and 256H18 (0.077%) (Fig. 4b). The morphology of sorted CD45$^+$ cells from 20D17, 256H18, and Hep-98A-1 iPS lines is shown in the Fig. 4c. The morphologies of iPS-derived CD45$^+$ and Ter119$^+$ cells were similar to that of CD45$^+$ and Ter119$^+$ cells differentiated from CCE ES cells. Taken together, Hep-98A-1 iPS cells generated the highest percentage of CD45$^+$ myeloid lineage cells, while the 178B5 iPS line generated the highest percentage of Ter119$^+$ erythroid lineage cells.

Discussion

iPS cell lines are grossly similar to ES cells in terms of morphology, pluripotency, gene expression patterns and

epigenetic status [1, 2]. However, here we demonstrated variation among six iPS cell lines in terms of differentiation capacity. MEF-derived 20D17, 178B5 and 492B4 iPS cells resembled CCE ES cells in terms of cell morphology in feeder-free culture, the number and size of EBs, and differentiation into mesoderm, but adult-derived iPS cell lines 256H18, Hep-98A-1, and Stm-99-1 differed in some properties. This tendency was independent of *c-Myc* gene transduction and Nanog/Fbx15 selection. These findings suggest that cell origin affects differentiation capacity of iPS cells and those embryonic cells are more capable of differentiation into mesodermal cells and HCs. The six iPS lines analyzed here were not identical in either proliferation or differentiation into mesodermal cells during EB formation. The adult-derived iPS lines 256H18, Hep-98A-1, and Stm-99-1 proliferated and differentiated more slowly than did the MEF-derived iPS lines 20D17, 178B5, and 492B4. Compared to other iPS cells, the 20D17 and 178B5 lines were similar to CCE ES cells in the percentage of mesodermal cells, whether they were E-cadherin$^-$ PDGFRα^+ cells (defined as paraxial lateral mesodermal) or E-cadherin$^-$ Flk1$^+$ cells (defined as proximal lateral mesodermal). Taken together, these findings suggest that MEF-derived iPS cells resemble CCE ES cells in mesodermal cell differentiation during EB formation, but adult-derived iPS cells do not.

The three MEF-derived iPS lines analyzed were constructed using different combinations of transcription factors and gene delivery methods. It remains unclear whether *c-Myc* transduction alters differentiation of iPS cells into mesodermal cells and HCs. Thus, we also compared the three MEF-derived lines (492B4, 20D17, and 178B5) generated by ectopic expression of *Oct3/4, Sox2* and *Klf4* combined with wild type *c-Myc*, T58A *c-Myc* (an active form) or without *c-Myc*. We found that the number of mesodermal and undifferentiated cells expressing Nanog-GFP at day 9 of EB formation was not correlated with *c-Myc* transduction, suggesting that *c-Myc* does not function in mesodermal differentiation capacity of iPS cells. This result is similar to reports that the neuronal potential of iPS lines is not correlated with *c-Myc* transduction [21]. However, we found that *c-Myc* transduction affected the hematopoietic potential of iPS cells. 20D17 iPS cells showed more potent myeloid differentiation, while 178B5 iPS cells showed more potent erythroid differentiation, although the origin of the cells and the combination of transduced genes used to create them were same except for *c-Myc*. Taken together, *c-Myc* transduction does not alter differentiation into mesodermal cells but does affects hematopoietic potential of MEF-derived iPS lines. Moreover, we demonstrate that among MEF-derived iPS cells, the efficiency of myeloid and erythroid cell differentiation was the lowest in 492B4 iPS cells. 492B4 iPS cells differ from 20D17 and 178B5 iPS cells in the method of gene delivery. In 492B4 iPS cells, MEFs were repeatedly transfected with plasmids carrying *Oct3/4*, *Sox2*, *Klf4*, and wild type *c-Myc* in order to attain sufficiently high expression levels [5]. Although 492B4 cells expressed Nanog-GFP after several passages without feeder layers and formed a significant number of EBs, the level of transcription factors expressed might alter their hematopoietic potential.

Fig. 3 Mesodermal cells derived from CCE ES/iPS cells. **a** The percentage of mesodermal cells (E-cadherin$^-$ Flk1$^+$ cell) at days (d) 4, 5, and 6 of EB culture was analyzed by flow cytometry. Like CCE ES cells, mesodermal cells derived from 20D17, 178B5, 492B4, and 256H18 iPS cells gradually decreased in number from days 4 to 6. **b** Percentages of E-cadherin$^-$ PDGFRα^+ and E-cadherin$^-$ PDGFRα^- population in EBs. **c** Summary of the total number of E-cadherin$^-$ Flk1$^+$ and E-cadherin$^-$ PDGFRα^+ (mesoderm and paraxial lateral mesoderm, respectively) cells. 20D17 and 178B5 iPS lines gave highest total cell number of E-cadherin$^-$ Flk1$^+$ cells at day 4, while 492B4, 256H18, Hep-98A-1, and Stm-99-1 iPS lines yielded highest total number of E-cadherin$^-$ Flk1$^+$ cells at day 5

We also observed that capacity to differentiate into HCs is related to somatic cell origin. Among the iPS six lines evaluated, Hep-98A-1 cells generated the highest percentage of CD45$^+$ myeloid cells and 178B5 cells generated the highest number of Ter119$^+$ erythroid cells. Moreover, Hep-98A-1 and Stm-99-1 iPS cells had greater potential to differentiate into erythroid cells than did 256H18, but showed no significant difference in the percentage of CD45$^+$ HCs. This suggests that iPS cell origin affects hematopoietic potential. However, DsRed, which is expressed in 256H18 cells, is reportedly more toxic to mouse ES cells than is GFP [22], suggesting that it also could affect hematopoietic potential.

A proposed use for iPS cells is to generate patient-specific lines from tissues from children or adults to serve as a source for HCs for transplantation: for example, it has been demonstrated that transplantation of HCs derived from autologous iPS cells could be used to treat humanized sickle cell anemia in mice [23]. iPS cells could also serve as a source of mature blood cells for transfusion. Moreover, disease-specific iPS cells may be useful to analyze mechanisms underlying hematological disease [24]. Finally, the efficacy and toxicity of a drug could be screened with iPS cells. Here, we demonstrate that MEF-derived 20D17 and 178B5 iPS cell lines have enhanced hematopoietic potential. A skin-derived iPS cell line is preferable to lines derived from other tissues in terms of access. It will be necessary to develop adult somatic cell-derived iPS cell lines that can differentiate into HCs more efficiently in the near future.

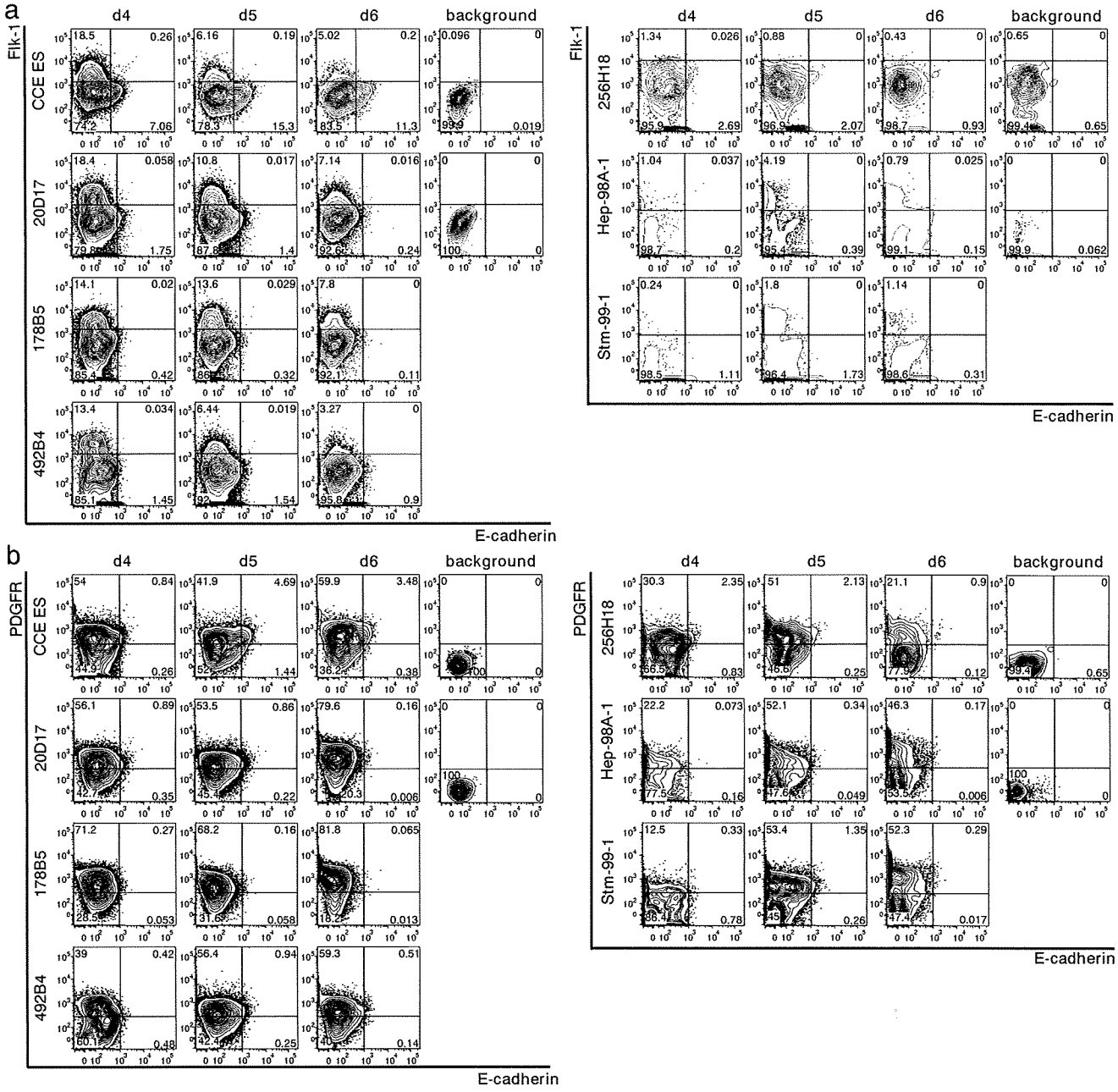
a
d4
d5
d6
background
Flk-1
CCE ES
20D17
178B5
492B4
256H18
Hep-98A-1
Stm-99-1
E-cadherin
b
PDGFR
E-cadherin
c
E-cadherin- Flk1+
E-cadherin- PDGFRα+
cell number x 10^3
CCE ES
20D17
178B5
492B4
256H18
Hep-98A-1
Stm-99-1

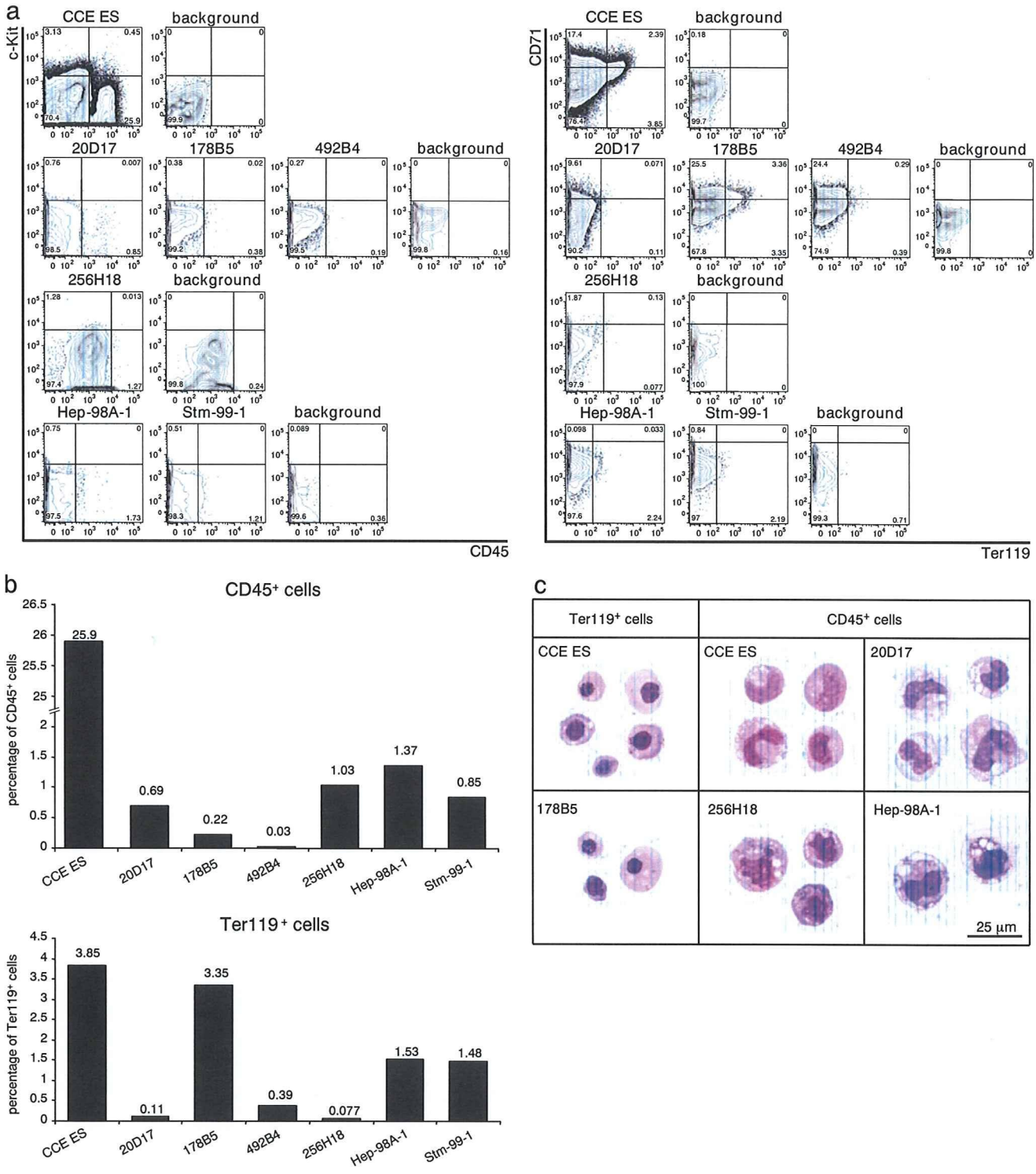

Fig. 4 Hematopoietic potential of iPS cells. **a** Hematopoietic progenitors (c-Kit$^+$ CD45$^+$), myeloid (CD45$^+$), and erythroid cells (CD71$^+$ and Ter119$^+$) in day 9 EBs derived from CCE ES cells and six iPS lines. To induce HCs, SCF, IL-3, and EPO were added to the culture. **b** Summary percentages of CD45$^+$ myeloid and Ter119$^+$ erythroid cells. **c** Morphologies of CD45$^+$ and Ter119$^+$ cells differentiated from CCE ES and iPS lines. Cells were sorted by flow cytometry and stained with May-Giemsa

Acknowledgements This research was partially supported by the Ministry of Education, Science, Sports and Culture. Dr. Kulkeaw Kasem was supported by a scholarship from the Ajinomoto Foundation. We thank Dr. Keisuke Okita, Ms. Tomoko Yokoo, and Mr. Tatsuya Sasaki for technical support. All iPS cell lines were kindly provided by Dr. Shinya Yamanaka.

Conflict of Interest All disclosures will be published if the manuscript is accepted.

References

1. Takahashi, K., & Yamanaka, S. (2006). Induction of pluripotent stem cells from mouse embryonic and adult fibroblast cultures by defined factors. *Cell, 126*, 663–675.
2. Okita, K., Ichisaka, T., & Yamanaka, S. (2007). Generation of germ-line competent induced pluripotent stem cells. *Nature, 448*, 313–317.
3. Nakagawa, M., Koyanagi, M., Tanabe, K., Takahashi, K., Ichisaka, T., Aoi, T., et al. (2008). Generation of induced pluripotent stem cells without Myc from mouse and human fibroblasts. *Nat Biotechnol, 26*, 101–106.
4. Stadtfeld, M., Brennand, K., & Hochedlinger, K. (2008). Reprogramming of pancreatic beta cells into induced pluripotent stem cells. *Curr Biol, 18*, 890–894.
5. Okita, K., Nakagawa, M., Hyenjong, H., Ichisaka, T., & Yamanaka, S. (2008). Generation of mouse induced pluripotent stem cells without viral vectors. *Science, 322*, 949–953.
6. Aoi, T., Yae, K., Nakagawa, M., Ichisaka, T., Okita, K., Takahashi, K., et al. (2008). Generation of pluripotent stem cells from adult mouse liver and stomach cells. *Science, 321*, 699–702.
7. Hanna, J., Markoulaki, S., Schorderet, P., et al. (2008). Direct reprogramming of terminally differentiated mature B lymphocytes to pluripotency. *Cell, 133*, 250–264.
8. Ye, Z., Zhan, H., Mali, P., Dowey, S., Williams, D. M., Jang, Y. Y., et al. (2009). Human-induced pluripotent stem cells from blood cells of healthy donors and patients with acquired blood disorders. *Blood, 114*, 5473–5480.
9. Takenaka, C., Nishishita, N., Takada, N., Jakt, L. M., & Kawamata, S. (2010). Effective generation of iPS cells from $CD34^+$ cord blood cells by inhibition of p53. *Exp Hematol, 38*, 154–162.
10. Lengerke, C., Grauer, M., Niebuhr, N. I., Riedt, T., Kanz, L., Park, I. H., et al. (2009). Hematopoietic development from human induced pluripotent stem cells. *Ann NY Acad Sci, 1176*, 219–227.
11. Doetschman, T. C., Eistetter, H., Katz, M., Schmidt, W., & Kemler, R. (1985). The in vitro development of blastocyst-derived embryonic stem cell lines: formation of visceral yolk sac, blood islands and myocardium. *J Embryol Exp Morphol, 87*, 27–45.
12. Wiles, M. V., & Keller, G. (1991). Multiple hematopoietic lineages develop from embryonic stem (ES) cells in culture. *Development, 111*, 259–267.
13. Keller, G., Kennedy, M., Papayannopoulou, T., & Wiles, M. V. (1993). Hematopoietic commitment during embryonic stem cell differentiation in culture. *Mol Cell Biol, 13*, 473–486.
14. Nakano, T., Kodama, H., & Honjo, T. (1994). Generation of lymphohematopoietic cells from embryonic stem cells in culture. *Science, 265*, 1098–1101.
15. Nakano, T., Kodama, H., & Honjo, T. (1996). In vitro development of primitive and definitive erythrocytes from different precursors. *Science, 272*, 722–724.
16. Nishigawa, S. I., Nishigawa, S., Hirashima, M., Matsuyoshi, N., & Kodama, H. (1998). Progressive lineage analysis by cell sorting and culture identifies FLK1+ VE-caherin+ cells at a diverging point of endothelial and hemopoietic lineage. *Development, 125*, 1747–1757.
17. Flamme, I., Breier, G., & Risau, W. (1995). Vascular endothelial growth factor (VEGF) and VEGF receptor 2 (flk-1) are expressed during vasculogenesis and vascular differentiation in the quail embryo. *Dev Biol, 169*, 699–712.
18. Huber, T. L., Kouskoff, V., Fehling, H. J., Palis, J., & Keller, G. (2004). Haemangioblast commitment is initiated in the primitive streak of the mouse embryo. *Nature, 432*, 625–630.
19. Choi, K., Kennedy, M., Kazarov, A., Papadimitriou, J. C., & Keller, G. (1998). A common precursor for hematopoietic and endothelial cells. *Development, 125*, 725–732.
20. Fehling, H. J., Lacaud, G., Kubo, A., Kennedy, M., Robertson, S., Keller, G., et al. (2003). Tracking mesoderm induction and its specification to the hemangioblast during embryonic stem cell differentiation. *Development, 130*, 4217–4227.
21. Miura, K., Okeda, Y., Aoi, T., et al. (2009). Variation in the safety of induced pluripotent stem cell lines. *Nat Biotechnol, 27*, 743–745.
22. Hadjantonakis, A. K., Macmaster, S., & Nagy, A. (2002). Embryonic stem cells and mice expressing different GFP variants for multiple non-invasive reporter usage within a single animal. *BMC Biotechnol, 2*, 11.
23. Hanna, J., Wernig, M., Markoulaki, S., et al. (2007). Treatment of sickle cell anemia mouse model with iPS cells generated from autologous skin. *Science, 318*, 1920–1923.
24. Park, I. H., Arora, N., Huo, H., et al. (2008). Disease-specific induced pluripotent stem cells. *Cell, 134*, 877–886.